Preliminary Liquid Hydrocarbon Potential Assessment of the Doig Formation, Northeastern British Columbia and West-Central Alberta, Based on Thickness, Organic Richness and Maturity

P.L. Silva, The University of British Columbia, Vancouver, BC, pablols@alumni.ubc.ca

R.M. Bustin, The University of British Columbia, Vancouver, BC

Silva, P.L. and Bustin, R.M. (2018): Preliminary liquid hydrocarbon potential assessment of the Doig Formation, northeastern British Columbia and west-central Alberta, based on thickness, organic richness and maturity; *in* Geoscience BC Summary of Activities 2017: Energy, Geoscience BC, Report 2018-4, p. 39–50.

Introduction

The Triassic section is the richest interval of the Western Canada Sedimentary Basin (WCSB) with respect to volume of oil per volume of rock (Marshall et al., 1987). Historically, the Doig and the underlying Montney formations were viewed as source rocks for other conventional reservoirs in the basin, mainly in other Triassic and Cretaceous strata (Du Rochet, 1985; Creaney and Allan, 1990; Riediger et al., 1990; Edwards et al., 1994). The Lower to Middle Triassic Doig Formation of the WCSB extends continuously across northeastern British Columbia (BC) and west-central Alberta (Figure 1). More recently, the Doig Formation has been recognized as an important unconventional reservoir for gas and natural-gas liquids (NGL), with estimates of total gas in place ranging from 1.1 to 5.6 trillion m^3 (Walsh et al., 2006). However, little is currently known about the unconventional portion of the Doig, which being a relatively new play is much less studied and understood than the Montney Formation. Basin-scale studies that focus on the entire Doig succession and the regional variation in its properties are notably absent in the literature.

The goal of the ongoing research project reported herein is to evaluate the potential of the Doig Formation through a petroleum system analysis (PSA), with focus on the distribution of producible liquids. The PSA is based on the quantification and mapping of source-rock properties, characterization of reservoir properties such as storage capacity and producibility, and backstrip modelling of the basin to reconstruct and determine the timing of thermogenic hydrocarbon generation, migration, expulsion and retention. This paper presents preliminary findings on the aspect dealing with the source-rock properties of the Doig Formation. Organic matter type, abundance and level of thermal maturity are the primary factors controlling the quantity and type of hydrocarbons generated (Welte and Leythaeuser, 1983). Combined with the spatial distribution of thickness, they are the most fundamental properties for assessing the potential of a source-rock reservoir.

This publication is also available, free of charge, as colour digital files in Adobe Acrobat® PDF format from the Geoscience BC website: http://www.geosciencebc.com/s/SummaryofActivities.asp.

Geological Framework

The Doig was deposited in the Middle Triassic, between the Anisian and Ladinian, and is part of the Diaber Group with the underlying Montney Formation (Figure 2). The sedimentation in the Triassic of the WCSB is marked by a transition from carbonate-dominated intra-cratonic and passive-margin conditions, predominant during the Paleozoic, to a siliciclastic-dominated relatively active embryonic foreland basin. The structural elements that influenced the distribution of the interval were the underlying Devonian Leduc reef and the Mesozoic reactivation of the Mississippian Dawson Creek graben complex (Marshall et al., 1987; Davies, 1997). The Doig Formation consists of mudstone, siltstone and subordinate sandstone, bioclastic packstone and grainstone, deposited under marine conditions in environments ranging from shoreface through offshore (Evoy and Moslow, 1995). The Doig can be informally subdivided into three units, as proposed by Chalmers and Bustin (2012): the basal unit, Doig A, corresponding to the also informal but widely used Doig Phosphate Zone (DPZ), composed of organic-rich radioactive dark mudstone with common phosphate granules and nodules, and generally very distinguishable in well logs by its high gamma-ray signature; the intermediate Doig B, primarily composed of medium to dark grey argillaceous siltstone and mudstone intercalated with localized sandstone; and the upper Doig C, composed of relatively organic-lean siltstone and argillaceous fine sandstone.

Methods

Cuttings samples from the Doig Formation were analyzed for total organic carbon (TOC) and temperature of maximum rate of hydrocarbon generation (T_{max}), as well as other standard pyrolysis-derived parameters. Existing pyrolysis data for the Doig in the public domain were compiled and thoroughly reviewed for consistency. As opposed to public

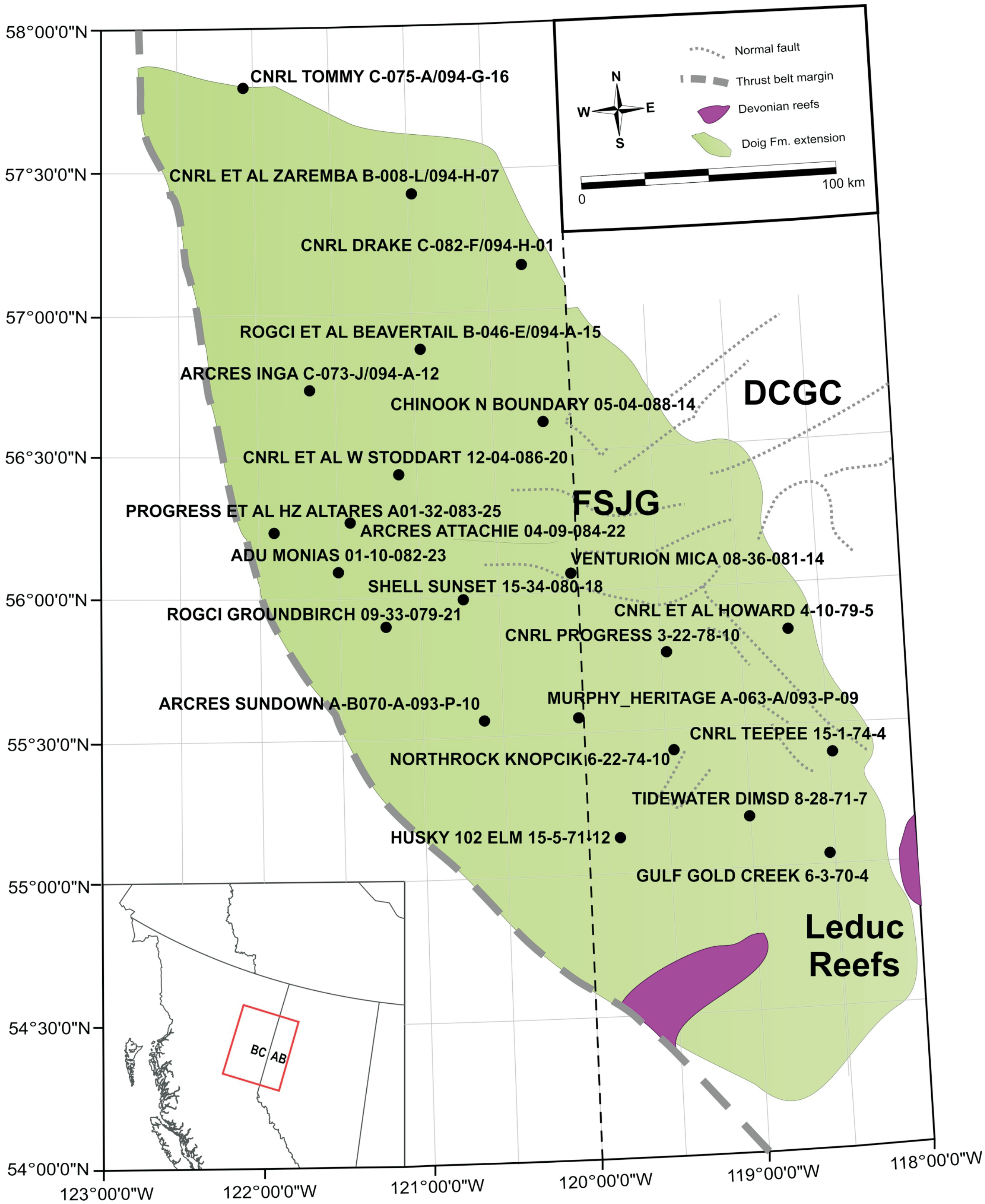

Figure 1. Location of the Doig Formation, main structural elements and wells analyzed in the study area in northeastern British Columbia and west-central Alberta. Abbreviations: DCGC, Dawson Creek graben complex; FSJG, Fort St. John graben.

data, for which no pyrograms or signal quality indicators were available, the data generated for this study was ranked according to signal quality and thus served as high-confidence control points, against which publicly available data was then compared. Between the public data and the analyses conducted for the purpose of this study, nearly 1500 data points from approximately 200 wells were used. The TOC from pyrolysis was used to derive and calibrate continuous TOC logs from compressional sonic slowness and resistivity well logs for all the wells. These logs were calibrated to the laboratory data to map the spatial distribution of the average values in the sequence. Structural, thickness, average TOC and maturity maps were then created and interpreted, with a focus on defining thick organic-rich areas in the liquid-hydrocarbon–rich generation window.

Pyrolysis

A total of 252 cuttings samples from 24 wells distributed across the entire extent of the Doig Formation were analyzed using the whole-rock pyrolysis method. The samples were selected at an average vertical spacing of 10 m and prepared as bulk rock samples (i.e., not high-graded toward clay-rich fractions). This decision was made in order to avoid overestimation of TOC, which is expected to have a positive correlation with clay; however, the clear trade-off was that the decision was made at the expense of a more pronounced kerogen conversion (S2) peak, and hence a better quality T_{max} value. The analyses were performed using a HAWK™ instrument from Wildcat Technologies with the standard pyrolysis method after Espitalié et al. (1977). Pyrograms were individually reviewed and the T_{max} values were ranked in quality according to the intensity and sharpness of S2. This resulted in the exclusion of 38% of the data for the purpose of maturity assessment as they were deemed unusable, due to being overmature or having low TOC content. Almost 26% of the data were ranked as 'poor' and thus have a low degree of reliability; the remaining 36% of the data was ranked 'good' or better.

A total of 1200 pyrolysis analyses for 170 wells from the public domain were compiled. Due to the unavailability of pyrograms, these data points were reviewed for consistency within each well and for regional agreement. From these data, 12% were beyond a reasonable range expected for T_{max} (400 to 550 °C); another 28% were considered outliers due to either deviating more than 5 °C from the well average or, in the case of wells with less than three data points, disagreeing with the regional trend so as to create bull's-eye patterns on the map. The remaining data were internally and/or regionally consistent, and thus used in the mapping.

Well-Log–Derived TOC

In regional studies involving a large number of wells, laboratory TOC data is sparse relative to the large volume being studied and therefore is of limited utility for regional mapping. Various methods have been developed for extrapolating laboratory data and creating a continuous record of TOC through the entire wellbore using well logs. The most commonly used logs are bulk density, compressional sonic slowness, resistivity and gamma ray. Whereas the use of sonic and density is based on kerogen having substantially lower density than the mineral matrix, gamma ray works on the assumption that organic matter has an affinity with uranium. Because well logs are sensitive to various changes in rock and fluid properties, and thus show non-unique responses, the most dependable methods for estimating TOC

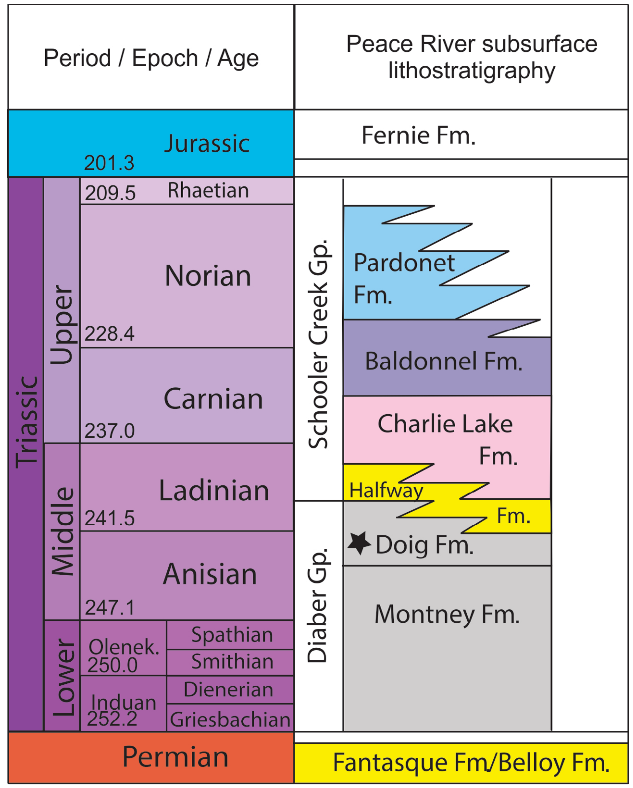

Figure 2. Stratigraphic chart of the Triassic, illustrating lithostratigraphic and chronostratigraphic relationships of the Peace River arch, northeastern British Columbia (after Golding et al., 2016). Abbreviations: Fm., Formation; Gp., Group; Olenek., Olenekian.

rely on a combination of sonic or density with resistivity. For the purpose of this study, two such methods were tested, one described in Passey et al. (1990) and the other in Carpentier et al. (1991), the latter also known as the CARBOLOG® method. Their individual calculations and assumptions differ slightly; however they both use sonic and resistivity in tandem, relying on the slower acoustic velocity of kerogen in less mature rocks and the increase in resistivity with maturity due to generation of hydrocarbons, which displace connate brine. The ΔlogR method proposed in Passey et al. (1990) is computed in two steps: firstly, for every depth, the separation between the sonic and resistivity curves, or ΔlogR, is calculated according to the equation

$$\Delta \log R = \log\left(\frac{R_t}{R_b}\right) + 0.02 \times (\Delta t - \Delta t_b) \quad (1)$$

where R_t and R_b are the true formation resistivity and the baseline resistivity in non-source, clay-rich rocks in ohm·m, respectively; and Δt and Δt_b are formation slowness and baseline slowness in non-source, clay-rich rocks in microseconds per metre (µs/m), respectively. In this study the values used for R_b and Δt_b were 23 ohm·m and 171 µs/m (52 µs/ft.), respectively.

Secondly, TOC was calculated using the formula

$$TOC = (\Delta \log R) \times 10^{(2.297 - 0.1688 \times LOM)} \quad (2)$$

as a function of ΔlogR and level of maturity (LOM), which in turn was calculated for all the wells as a linear function of depth of burial. The calculated LOM values are between 2 and 8 with a median of 4.6.

The CARBOLOG® method TOC computation is also based on sonic slowness and resistivity and can be represented in a crossplot of sonic slowness on the x axis and the inverse of the square root of resistivity on the y axis (Figure 3). The volume of organic matter is calculated according to the distance between lines of equal TOC defined by three end points. End members are defined as matrix, organic matter and brine. Both matrix and organic matter points are assumed to be infinitely resistive and thus lie along the x axis, where y equals zero. The matrix point and the slope of the 0% organic matter line are determined by the distribution of the data, which is naturally bound by a linear slope when plotted as described. The projection of the line on the opposite end of the pure-matrix point is the theoretical pure-brine point. The lines of same organic-matter content are then drawn parallel to, and equally spaced from, the first line to a theoretical 100% organic-matter point on the slow-velocity side of the crossplot, which is determined in an empirical, iterative way.

The TOC is then calculated for each depth frame according to their distance between the 100% matrix and organic-matter lines in the Cartesian plane. Due to the difference in density of mineral matrix and kerogen, the values calculated correspond to volume percentage and hence must be converted into weight fraction as per the equation

$$\mathrm{TOC} = V_{om} \times \left(\frac{\rho_{om}}{\rho_m}\right) \times \frac{1}{k} \qquad (3)$$

where V_{om} is the volume percentage of organic matter, ρ_{om} and ρ_m are the densities of organic matter and mineral matrix, set as constant values at 1.2 and 2.71 g/cm^3, respectively; and k is a unitless organic-carbon conversion factor, with an empirically determined value of 1.25. The TOC calculated by both methods was extrapolated to approximately 200 wells that had slowness and resistivity logs available for the entire Doig interval, as well as pyrolysis laboratory data, to assess the accuracy of the methods and adjust the parameters where necessary. The parameters were adjusted iteratively to minimize the difference between laboratory and log TOC.

Mapping

Formation picks for the top and base of the Doig were obtained from the database in geoSCOUT™ for approximately one thousand wells. Due to the time-consuming nature of individually checking every well, quality control of formation picks for the purpose of this study was limited to repicking or deleting wells that caused bull's-eye patterns on the structural maps. Gross-thickness isochore maps were then calculated between the top of the Montney and top of

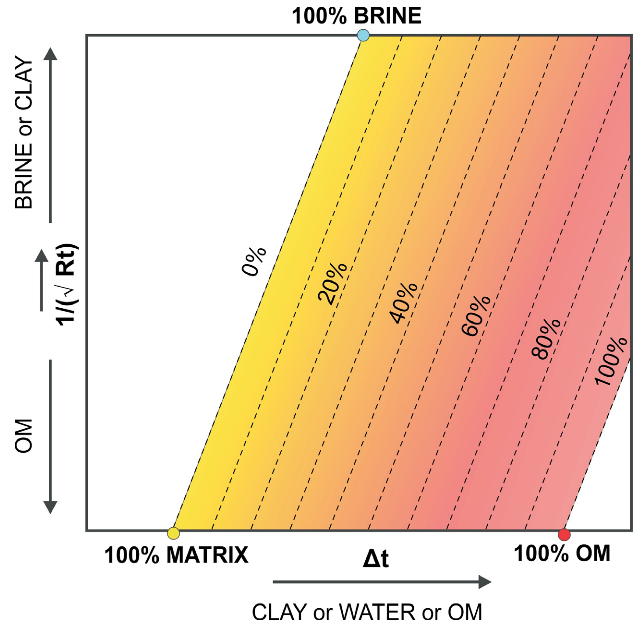

Figure 3. Crossplot showing a graphical representation of the CARBOLOG® method of total organic carbon (TOC) computation (dashed lines) in terms of three end members (poles) according to their compressional slowness and inverse of square root of resistivity relationship (after Carpentier et al., 1991), using well-log data from the Doig Formation, northeastern British Columbia and west-central Alberta. Abbreviations: OM, organic matter; Rt, true resistivity; Δt, compressional sonic slowness.

the Doig. Grids of the average CARBOLOG® method TOC values for the entire Doig interval in each well and T_{max} were created using simple regression kriging. The search radius for each grid was determined through experimental variograms at 25 km for TOC and 100 km for T_{max}. The larger radius for T_{max} is due to the smoother trend in maturity caused by the regional dip, relatively to the more random nature of TOC distribution. The map boundaries are the Doig subcrop edge to the northeast and the deformation front of the Cordilleran foreland fold-and-thrust belt to the southwest. Data in the deformation belt were not used at this stage, as it would require structural restoration to their original location relative to the undeformed portion.

Pyrolysis

The 80% confidence interval of TOC content for the Doig is between 0.8% and 4.8%, with a median of 2% and a maximum of 14.7% (Figure 4). However, this maximum is from the public data and may not be completely reliable since it was not possible to obtain their raw files. The highest value observed in the samples analyzed for this study is 8.6%. There is a large range of values for the hydrogen index (HI), spanning from nearly 0 to almost 500, over a wide range of thermal maturity from immature to overmature (Figure 5). This range of HI values for similar T_{max} values through the oil window suggests that multiple types of kerogen are present in the Doig, from type II, through type II-III to type III. In the samples analyzed for this study, which were properly calibrated and quality checked, and hence carry a higher degree of confidence, there was only type II-III and type III kerogen observed. This observation differs substantially from other studies that found mostly type II kerogen in the Doig (Riediger et al., 1990; Ibrahimbas and Riediger, 2004; Walsh et al., 2006). Thermal maturity within wells does not show any increasing trend with depth, despite section thicknesses in excess of 300 m.

TOC Transform

Overall, both the CARBOLOG® method and the method proposed by Passey et al. (1990) had acceptable results in estimating TOC content, on average showing good agreement with the laboratory data. The quality of the match was assessed by subtracting the log-derived TOC value from the laboratory-derived TOC (Figure 6). If the method was completely accurate, the subtraction would be null. Due to log resolution, depth shifts, imperfect assumptions, analytical errors and other factors, the subtraction results in a residual error. Although both methods employed to estimate TOC from well logs use resistivity and compressional sonic slowness, CARBOLOG® yielded superior results when compared to the ΔlogR (Passey et al., 1990) method. The median of the laboratory and log difference for the CARBOLOG® and ΔlogR (Passey et al., 1990) methods were 0.47 and 0.96, with standard deviations of 2.65 and 3.36, respectively (Figure 6). The larger average error and higher standard deviation for the ΔlogR (Passey et al., 1990) method is likely due to the fact that, unlike the CARBOLOG method, it weights resistivity higher relative to sonic and the resistivity logs have lower vertical resolution. Additionally, migrated hydrocarbons will tend to increase the resistivity above the baseline in cleaner rock types and hence result in erroneously high calculated TOC (Figure 7).

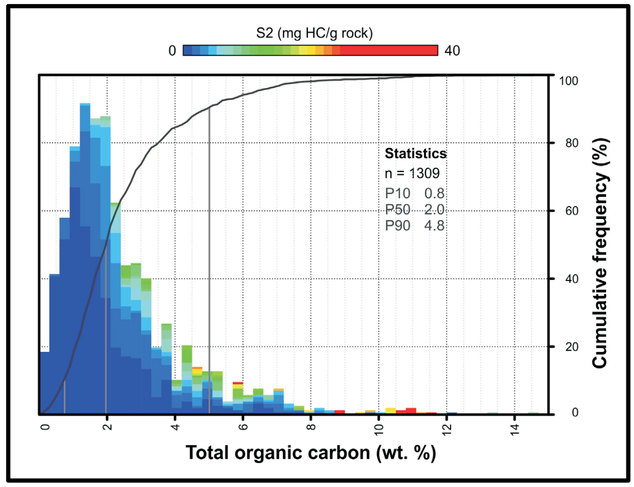

Figure 4. Histogram and key statistical parameters of all total organic carbon (TOC) from the public data and samples analyzed for this study of the Doig Formation, northeastern British Columbia and west-central Alberta, coloured by intensity of the kerogen conversion peak (S2). Abbreviations: n, sample size; P, probability.

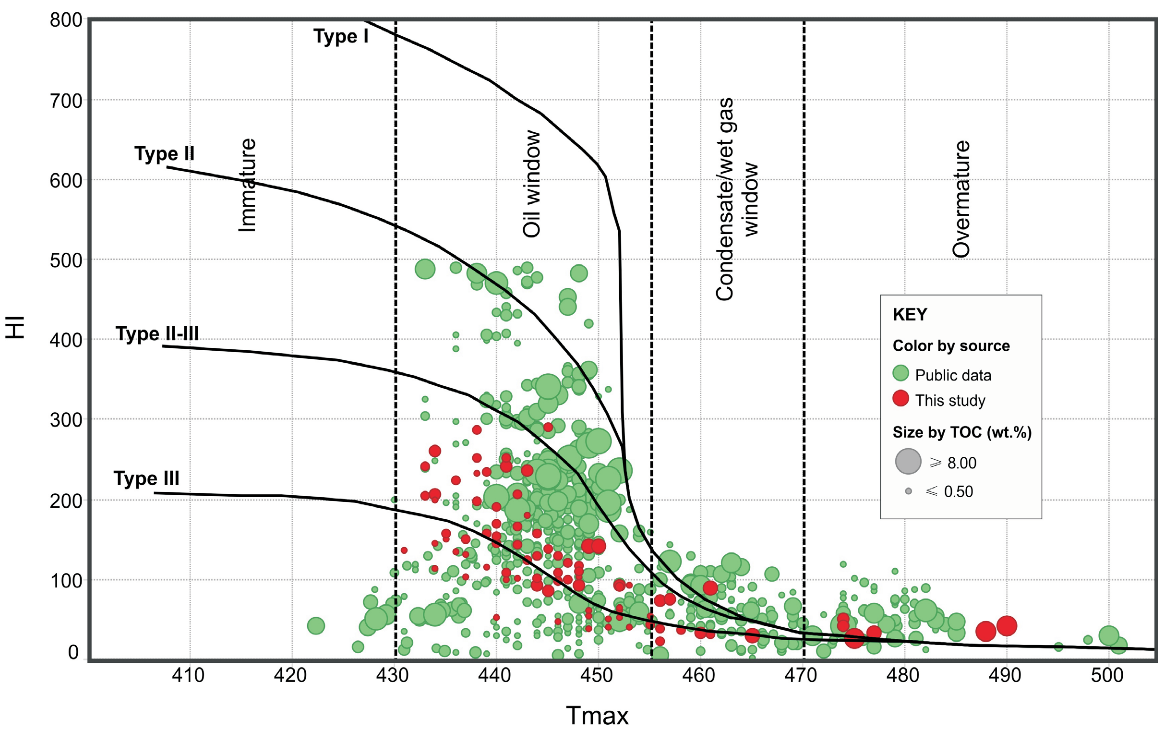

Figure 5. Hydrogen index (HI) versus temperature of maximum rate of hydrocarbon generation (T_{max}) of pyrolysis data from public domain and generated for this study of the Doig Formation, northeastern British Columbia and west-central Alberta, colour coded by data source and sized by total organic carbon (TOC). Only data points that either presented a good quality kerogen conversion peak (S2) or consistent T_{max} values are shown.

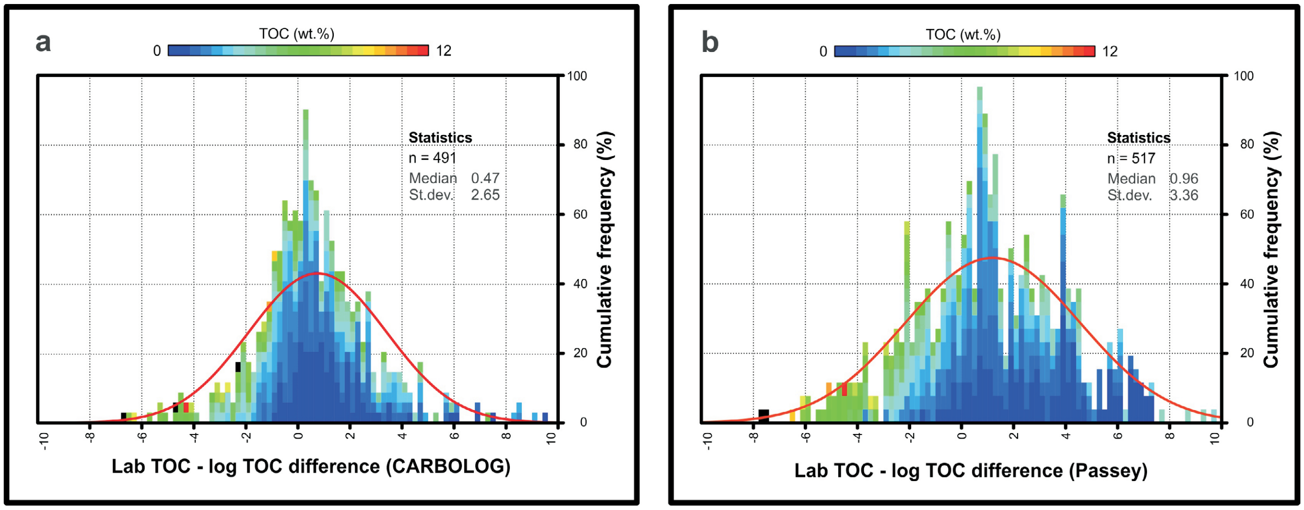

Figure 6. Histograms of the difference between laboratory- and log-derived (lab-log) total organic carbon (TOC) values from both **a)** the CARBOLOG® and **b)** the ΔlogR methods using data from the Doig Formation, northeastern British Columbia and west-central Alberta, showing a symmetric and narrow distribution centred about zero. Abbreviations: n, sample size; Passey, ΔlogR (Passey et al., 1990) method; St. dev., standard deviation.

Structure and Isochore

The top and base (top of the Montney Formation; Figure 2) structures of the Doig Formation are subparallel and follow the general southwest-trending dip of the Phanerozoic in the basin (Figure 8). A slight increase in dip angle is evident south of a line defined by the southern edge of the Monias and Progress oilfields. The dip of both top and base change from 0.4° in the northeast portion of the basin, to approximately 0.7° through a slope 40 km wide following the regional strike, and revert back to a gentler dip of 0.3° in the distal part of the basin. This relatively steep-dipping slope

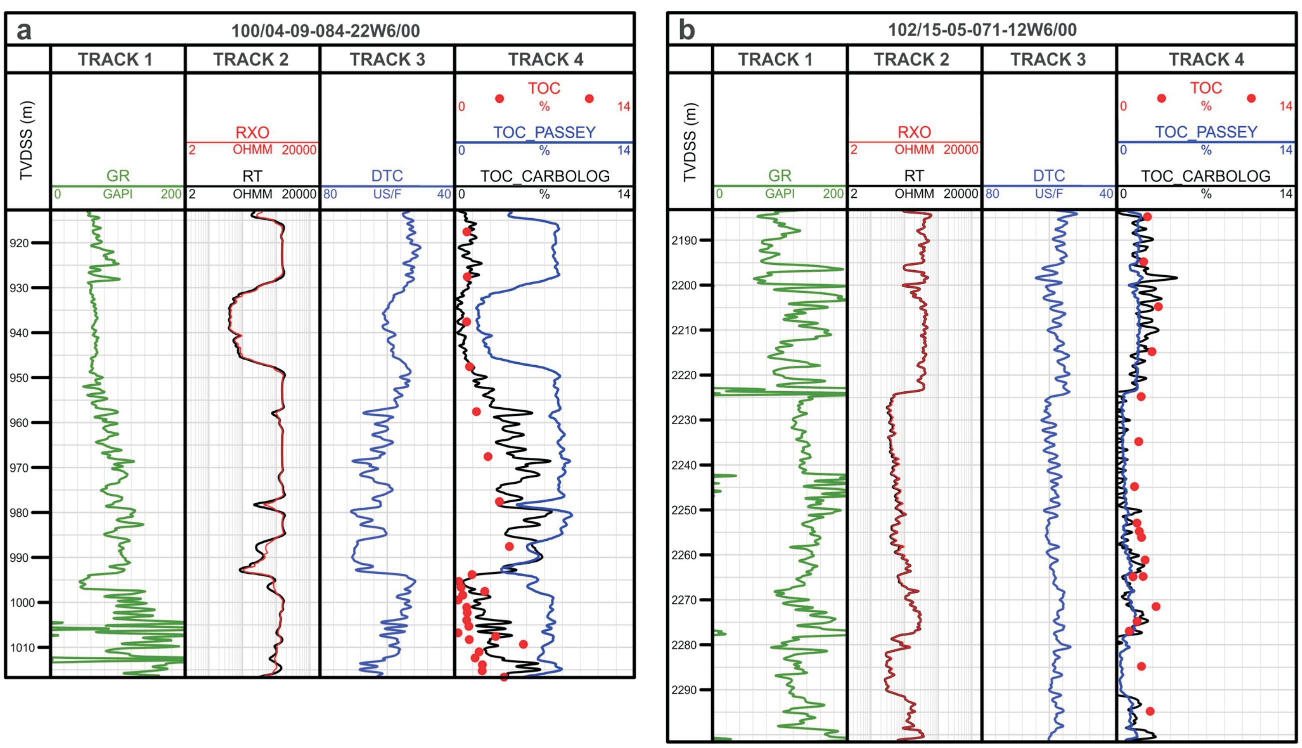

Figure 7. Log plots of two wells (a and b) in northeastern British Columbia and west-central Alberta showing, from left to right on each well: vertical depth below sea level (TVDSS), gamma ray (GR) in track 1, resistivity (RT) in track 2`, compressional sonic slowness (DTC) in track 3, total organic carbon (TOC) in track 4. CARBOLOG® TOC shows good agreement with laboratory data (red circles) in both wells, whereas the ΔlogR (Passey et al., 1990) method has a good match on well b, but largely overestimates TOC on well a.

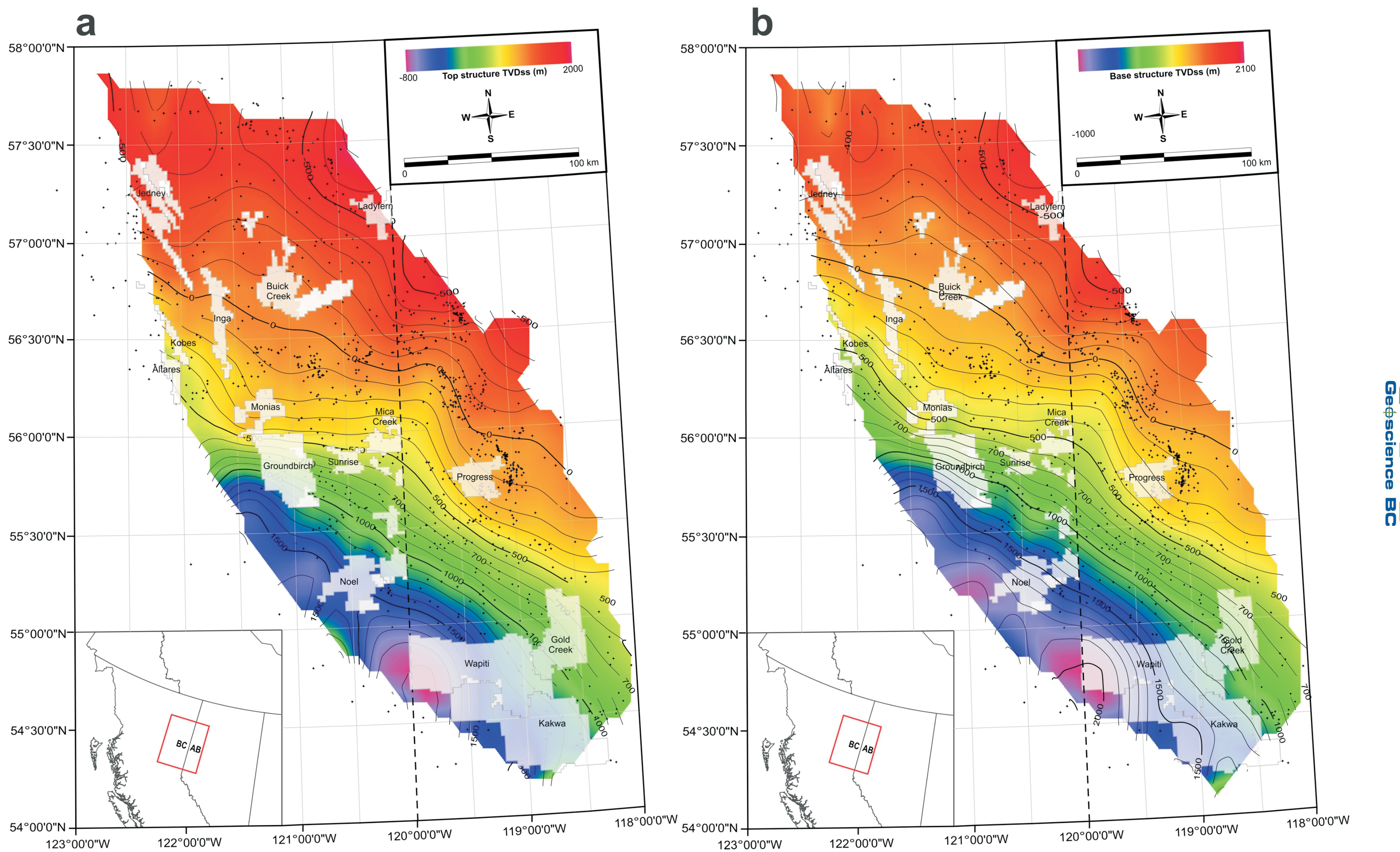

Figure 8. Structure maps of the Doig Formation **a)** top and **b)** base (Montney Formation top) in northeastern British Columbia and west-central Alberta, with elevations expressed in vertical metres below mean sea level (TVDss) permanent datum.

is interpreted as the paleoshelf break and likely represents an important facies boundary between coarser-grained shelf sediments to the northeast and finer-grained sediments to the southwest.

A southwest-trending linear feature of negative relief exists between the Mica Creek and Progress fields. This feature is approximately coincident with the Fort St. John graben complex (Figure 1) and is associated with increased accommodation space, as evidenced by the thickening of the Doig interval northwest of the Progress field (Figure 9). The trough may have also served as a sediment conduit into the deeper part of the basin showing anomalous thicknesses in excess of 160 m immediately southwest of the trough, around the vicinity of the Noel field in BC up to the border with Alberta. The average thickness of the Doig interval is 84 m with an 80% confidence interval between 25 and 175 m. Other regions of anomalous thicknesses in excess of 240 m are located in the west-central part of the basin, in a semi-circular shape around the Monias and Groundbirch fields and thickening to the west, and in the northwest of the Inga field.

The average interval TOC from CARBOLOG® has a background of 3% in weight, ranging from 1.2% to 7.5% in weight (Figure 10). One of the areas with the highest average TOC coincides with the anomalous thickness on, and immediately adjacent to, the depression associated with the Fort St. John graben. This area is bounded on both sides by regions of TOC lower than the background. Another area of high TOC associated with a thick gross interval occurs on and around the Sunrise oilfield, immediately east of the Groundbirch field. Elevated average TOC values are also observed with no association to increased thickness in the relatively shallow dipping platform near the Altares, Kobes, Inga and Buick Creek fields.

The maturity map reveals T_{max} values from the early oil window, using the zones for petroleum generation for type II kerogen from Dow (1977) as a reference, in the eastern and southwestern portions of the basin, through condensate/wet gas, to peak dry gas in the western edge against the deformation front (Figure 11). Approximately 76% of the area is in the oil window, with 22% in the condensate/wet gas and 2% in the dry gas window (Table 1). In terms of gross rock volume within each region, the numbers are slightly skewed toward condensate/wet gas and dry gas, as the thickness increases westward, so that approximately 60% of the total rock volume is in the oil window, 34% in the condensate/wet gas, and over 5% in the dry gas. Within the southern portion of the basin, on the eastern side of the Wapiti field, there is an area of increased maturity in the peak oil window. There is a broad area in the west-central region lying in the condensate/wet gas window, which roughly coincides with the alignment of the Jedney, Inga, Groundbirch and Sunrise fields.

Conclusions

The work presented here is based on a preliminary assessment of source-rock properties and will serve as the foundation for a PSA of the Doig Formation, incorporating an evaluation of its reservoir properties and a reconstruction of its thermal history through basin modelling. The data provide insights for evaluating the additional potential of currently developed areas as well as new prospects. The combination of maturity and thickness maps suggests that one third of the Doig gross rock volume lies within the condensate/wet gas window for type II kerogen. The vast majority of this area is in BC. By combining the isochore with the average TOC map, total carbon thickness maps may be calculated and used for further assessing hydrocarbon prospectivity.

Ongoing work will improve the quality of the results presented in this preliminary update, as well as integrate these data into a basin model. The picks for top and base of the Doig will be more thoroughly reviewed for consistency, improving the accuracy of the thickness maps. The DPZ top and its correlative surface will be picked across the entire distribution of the Doig, subdividing the mapping in two intervals. This subdivision will highlight differences in thickness and TOC distribution of the more organic-rich basal interval. The log-derived TOC estimation for this work was performed only in wells for which laboratory data was available, so that the quality of the model could be checked, and served as a proof of concept. Additional log-based TOC methods will be evaluated, and the existing models will be refined. With increased confidence in the models, all wells with a minimum log suite will ultimately be used in the mapping of TOC, resulting in a denser grid of data and a TOC map with enhanced resolution and accuracy. Historic production data will be integrated into the analysis and cross-correlated with the maturity maps. Integrating the production data will be particularly useful for the investigation of the influence of kerogen type on the type of hydrocarbons generated. If there are multiple types of kerogen present in the Doig, as pseudo-van Krevelen and T_{max} versus HI crossplots suggest, they are expected to play an important role in the type of hydrocarbon generated and produced. In that case, kerogen type will have to be taken into account when delineating liquid-rich areas, by means of defining regional trends in the type of kerogen and establishing correlations with lithofacies.

Acknowledgments

The authors would like to acknowledge financial support from Geoscience BC, Canadian Natural Resources Limited, Chevron Canada Limited, Devon Energy Corporation, Encana Corporation, geoLOGIC Systems ltd., Husky Energy Inc. and Trican Geological Solutions Ltd. This study would not have been possible without the generous lending

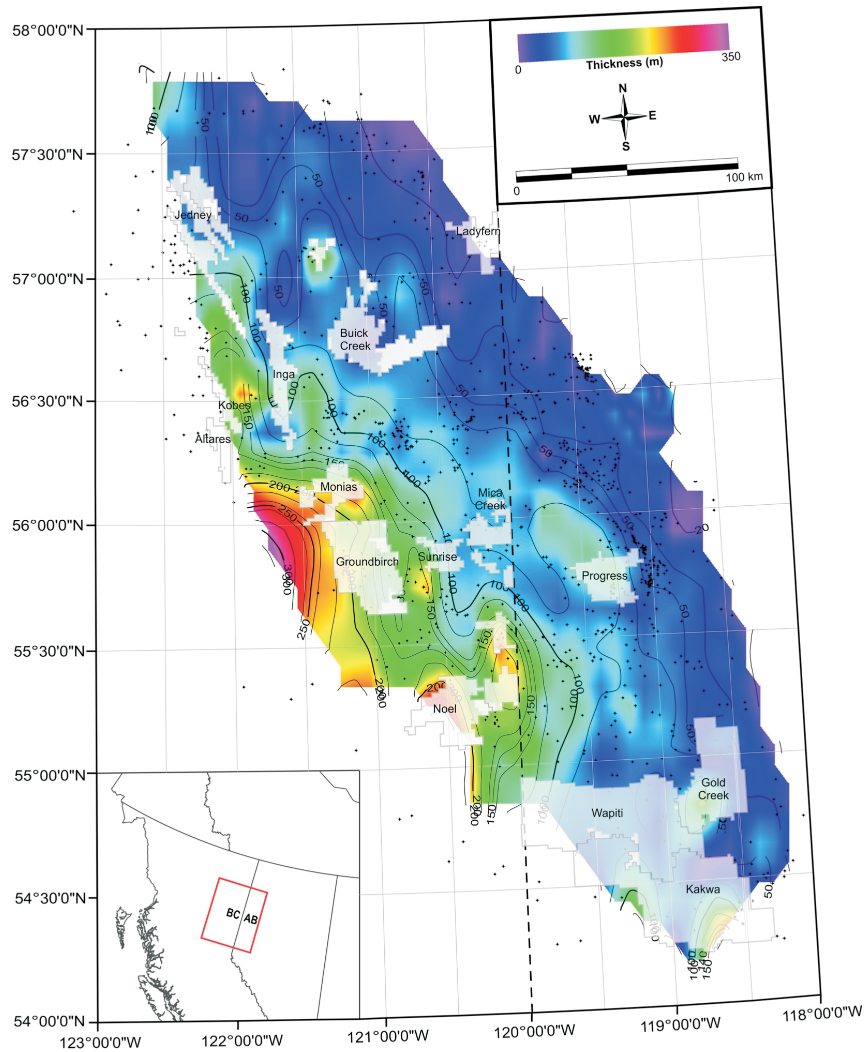

Figure 9. Gross isochore map of the Doig interval in northeastern British Columbia and west-central Alberta, with thicknesses expressed in metres.

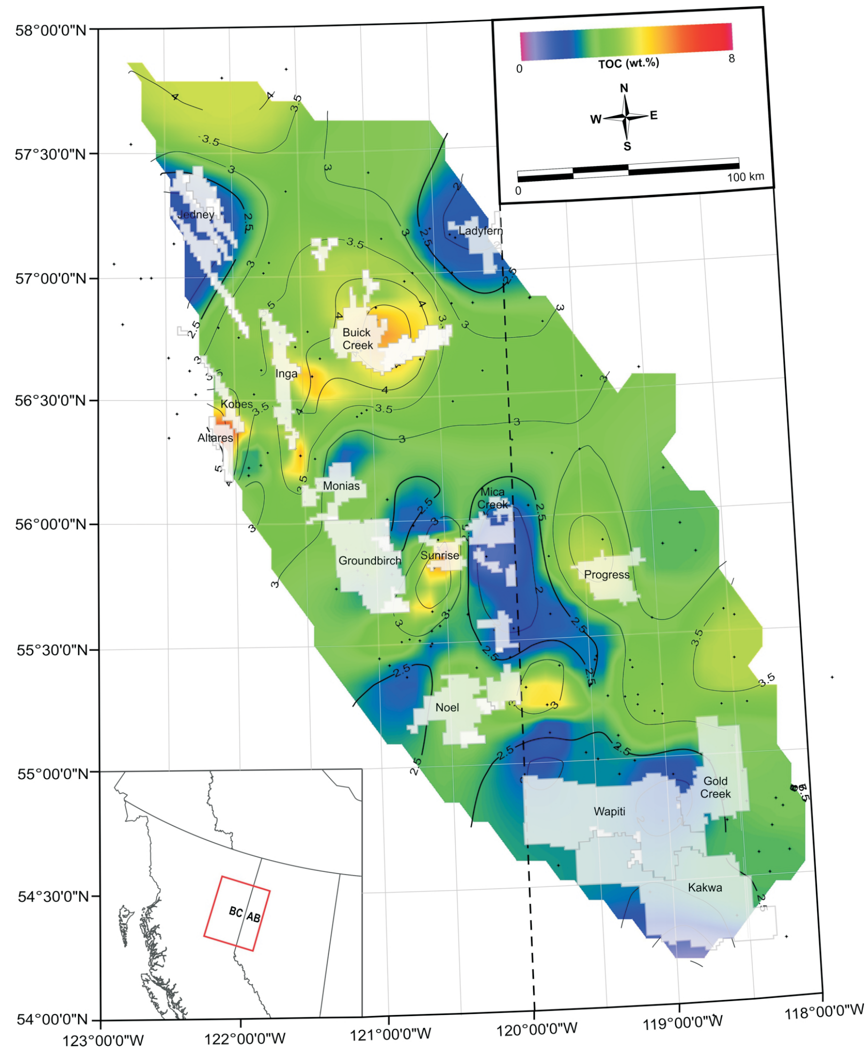

Figure 10. Average total organic carbon (TOC) map for the Doig interval in northeastern British Columbia and west-central Alberta, with TOC content expressed in weight percentage.

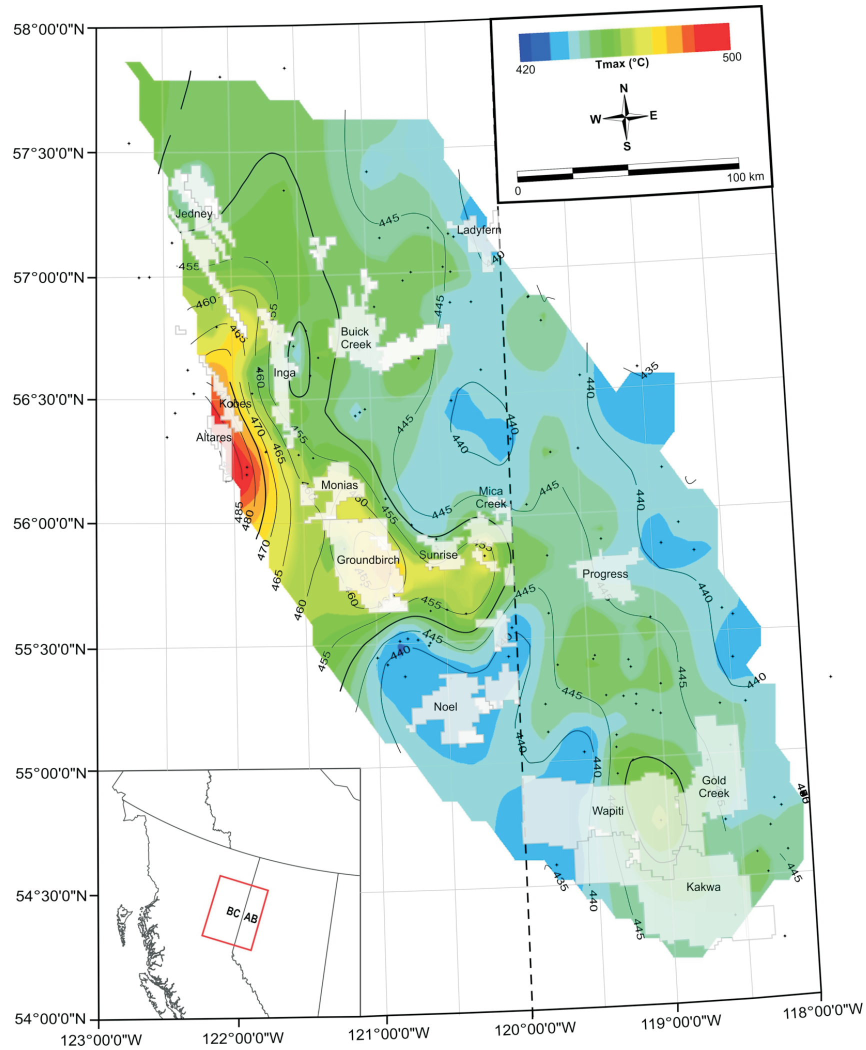

Figure 11. Generalized thermal maturity map of the Doig interval in northeastern British Columbia and west-central Alberta, expressed by temperature of maximum rate of hydrocarbon generation (T_{max}).

of instruments by, and valuable expertise of, Trican's staff, especially B. Nassichuk, C. Twemlow and S. Tu. Also essential for this study and greatly appreciated was the kind donation of software by geoLOGIC Systems ltd. and Paradigm Geophysical Canada Ltd. The authors would also like to thank D. Mare for his efforts in finding and compiling public domain data and, last but not least, they acknowledge the time and effort dedicated to the thorough review of the manuscript by E. Letham, Ph.D. candidate at The University of British Columbia.

Table 1. Area and gross rock volume of the Doig Formation in northeastern British Columbia and west-central Alberta, within each hydrocarbon generation window.

Window (Tmax)	Area ($x10^{10}$ m^2)	Area (%)	Volume ($x10^{12}$ m^3)	Volume (%)
Oil (430–455°C)	5.003	75.7	3.021	60.3
Condensate/wet gas (455–470°C)	1.448	21.9	1.717	34.3
Dry Gas (>470°C)	0.155	2.3	0.269	5.4

References

Carpentier, B., Huc, A.Y. and Bessereau, G. (1991): Wireline logging and source rocks – estimation of organic content by CARBOLOG® method; The Log Analyst, v. 32, no. 3, p. 279–297.

Chalmers, G.R.L. and Bustin, R.M. (2012): Geological evaluation of Halfway-Doig-Montney hybrid gas shale-tight gas reservoir, northeastern British Columbia; Marine and Petroleum Geology, v. 38 p. 53–72.

Creaney, S. and Allan, J. (1990): Hydrocarbon generation and migration in the Western Canada Sedimentary Basin; *in* Classic Petroleum Provinces, J. Brooks (ed.), Geological Society Special Publication 50, p. 189–203.

Davies, G.R. (1997): The Triassic of the Western Canada Sedimentary Basin: tectonic and stratigraphic framework, paleogeography, paleoclimate and biota; Bulletin of Canadian Petroleum Geology, v. 45, no. 4, p. 434–460.

Dow, W.G. (1977): Kerogen studies and geological interpretations; Geochemical Exploration Journal, v. 7, p. 79–99.

Du Rouchet, J. (1985): The origin and migration paths of hydrocarbons accumulated in the Lower Cretaceous sandstone “giant” tar accumulations of Alberta – Part II; Journal of Petroleum Geology, v. 8, no. 1, p. 101–114.

Edwards, D.E., Barclay, J.E., Gibson, D.W., Kvill, G.E. and Halton, E. (1994): Triassic strata of the Western Canada Sedimentary Basin; Chapter 16 *in* Geological Atlas of the Western Canada Sedimentary Basin, G.D. Mossop and I. Shetsen (ed.), Canadian Society of Petroleum Geologists and Alberta Research Council, Edmonton, Alberta, p. 257–275.

Espitalié, J., Madec, M. Tissot, B., Mennig, J.J. and Leplat, P. (1977): Source rock characterization method for petroleum exploration; Offshore Technology Conference, 2–5 May 1977, Houston, Texas, Paper 2935.

Evoy, R.W. and Moslow, T.F. (1995): Lithofacies associations and depositional environments in the Middle Triassic Doig Formation, Buick Creek Field, northeastern British Columbia; Bulletin of Canadian Petroleum Geology, v. 43, no. 4, p. 461–475.

Golding, M.L., Mortensen, J.K., Ferri, F., Zonneveld, J.-P., Orchard, M.J. and Rygel, M. (2016): Determining the provenance of Triassic sedimentary rocks in northeastern British Columbia and western Alberta using detrital zircon geochronology, with implications for regional tectonics; Canadian Journal of Earth Sciences, v. 53, no. 2, p. 140–155.

Ibrahimbas, A. and Riediger, C.L., (2004): Hydrocarbon source rock potential as determined by Rock- Eval 6/TOC pyrolysis, northeast British Columbia and northwest Alberta; *in* Summary of Activities, BC Ministry of Energy, Mines and Petroleum Resources, Oil and Gas Division, Resource Development and Geoscience Branch, p. 7–18.

Marshall, G.M., Noble, I.A. and Tang, R.C.W. (1987): Triassic/Jurassic fields; Chapter 7 *in* Geophysical Atlas of Western Canadian Hydrocarbon Pools, N.L. Anderson, L.V. Hills and D.A. Cederwall (ed.), Canadian Society of Exploration Geophysicists and Canadian Society of Petroleum Geologists, p. 187–215, URL <http://www.cspg.org/cspg/documents/Publications/Atlas/geophysical/L_Chap ter_7.pdf> [November 2016].

Passey, Q.R., Creaney, S., Kulla, J.B., Moretti, F.J. and Stroud, J.D. (1990): A practical model for organic richness from porosity and resistivity logs; American Association of Petroleum Geologists Bulletin, v. 74, no. 12, p. 1777–1794.

Riediger, C.L., Fowler, M. G., Brooks, P. W. and Snowdon, L. R. (1990): Triassic oils and potential Mesozoic source rocks, Peace River Arch area, Western Canada Basin; Organic Geochemistry, v. 16, no. 1–3, p. 295–306.

Walsh, W., Adams, C., Kerr, B. and Korol, J. (2006): Regional “shale gas” potential of the Triassic Doig and Montney formations, northeastern British Columbia; BC Ministry of Energy, Mines and Petroleum Resources, Oil and Gas Division, Resource Development and Geoscience Branch, Petroleum Geology Open File 2006-02, 19 p., URL <http://www2.gov.bc.ca/assets/gov/farming-natural-resources-and-industry/natural-gas-oil/petroleum-geoscience/petroleum-open-files/pgof20062.pdf> [November 2016].Welte, D.H. and Leythaeuser, D. (1983): Generation of hydrocarbons in source rocks; Naturwissenschaften, v. 70, p. 53–59.